*energies*

MDPI

*Article*

# Exergoeconomic and Environmental Evaluation of a Ground Source Heat Pump System for Reducing the Fossil Fuel Dependence: A Case Study in Rome

**Fabio Nardecchia *, Laura Pompei, Edoardo Egidi, Riccardo Faneschi and Giuseppe Piras**

Department of Astronautical, Electrical and Energy Engineering (DIAEE), Sapienza University of Rome, 00184 Rome, Italy; laura.pompei@uniroma1.it (L.P.); egidi.1795329@studenti.uniroma1.it (E.E.); faneschi.1796336@studenti.uniroma1.it (R.F.); giuseppe.piras@uniroma1.it (G.P.)

* Correspondence: fabio.nardecchia@uniroma1.it

**Abstract:** By 2050, the European Commission aims to achieve a 90% reduction in greenhouse gas emissions within the construction sector due to new targets set for greenhouse gases by the Commission. One of the most effective solutions for mitigating the environmental impact of buildings is to integrate renewable-energy systems such as air-to-water heat pumps or geothermal heat pumps. Several works in the literature investigated the advantages of heat pumps, particularly ground source heat pumps, for specific contexts. Furthermore, the evaluation can encompass not only energy considerations but also exergetic aspects, and this paper makes a significant contribution to the latter. The study presented here applies exergy analysis to a geothermal heat pump system that is interconnected with photo-voltaic and solar collector systems in a building located in Rome. Feasibility and environmental assessments were also conducted. It is evident that the exergy efficiency obtained is much lower than the energy efficiency. The heat pump demonstrates higher exergy efficiency by producing high-temperature thermal power compared to a constant dead state at relatively low temperatures. Following the heat pump, the adiabatic mixer exhibits the second highest exergy efficiency, trailed by two heat exchangers. Compared to a conventional plant case, the money saved is EUR 16,772 per year, translating to a Payback Period of 23 years. Furthermore, the average annual reduction in fossil fuel emissions is estimated at 26.2 metric tons of $CO_2$.

**Keywords:** energy renovation of buildings; exergy analysis; ground source heat pump; solar collector; photovoltaic plant; energy transition



**Citation:** Nardecchia, F.; Pompei, L.; Egidi, E.; Faneschi, R.; Piras, G. Exergoeconomic and Environmental Evaluation of a Ground Source Heat Pump System for Reducing the Fossil Fuel Dependence: A Case Study in Rome. *Energies* **2023**, *16*, 6167. https://doi.org/10.3390/en16176167

Academic Editors: Alessia Arteconi and Rafik Belarbi

Received: 18 July 2023
Revised: 8 August 2023
Accepted: 20 August 2023
Published: 24 August 2023



## 1. Introduction

Since 2010, the European Commission has established new targets for greenhouse gas emissions from the construction sector, aiming to reduce carbon dioxide equivalent emissions ($CO_2$eq) by 90% by 2050 [1]. According to the 2014/2015 European Work Program [2], it is projected that over 17% of the EU's energy-saving potential for 2050 will be dedicated to retrofitting buildings. Throughout the lifetime of a building, energy and raw materials are continuously utilized. As a results, the operation phase of the building requires significant in situ energy consumption, while the construction, operation, retrofit and demolition stages consume minor energy, alongside the production of building materials and technical equipment.

A critical strategy for enhancing building energy efficiency is recognizing that 60% of the energy consumption is attributed to space conditioning. This concern is particularly relevant in countries like Italy, where a majority of residential and commercial structures were erected prior to the implementation of stringent energy efficiency regulations. Numerous studies have emphasized the urgent need for comprehensive energy and environmental redesign of the entire urban district [3–6]. The integration of renewable energy systems,

such as air-to-water heat pumps or geothermal heat pumps (GSHP), represents the most effective solution, especially to mitigate the environmental impacts of buildings [7–12].

Exergy analysis is a thermodynamic analysis methodology that assesses the quality or value of the useful work generated by a system or process. In essence, exergy analysis evaluates a system's efficiency not only in terms of energy but also in terms of energy quality [13,14]. When comparing air–water and geothermal heat pumps using exergy analysis, key factors to consider encompass efficiency, heat source temperatures, and environmental effects. The exergy efficiency of a heat pump indicates the ratio of useful work produced to the total work supplied to the system. Exergy efficiency is influenced by variables such as the heat source temperature and the temperature of the heating or cooling fluid. In the scientific community, the comparison of exergy efficiency has been extensively studied over time. As early as 1994, Groll and Braun [15] conducted a comparative exergy analysis between air–water and geothermal heat pumps, assessing exergy efficiency and comparing outcomes between the two systems. Ibrahim and Al-Sulaiman [16] performed an exergy analysis of a geothermal heat pump system, evaluating exergy efficiency and identifying key factors affecting system performance. Conversely, Sopian and Yatim [17] focused on the exergy efficiency of heat pump systems used for drying purposes, examining different refrigeration cycles and evaluating performance in terms of exergy. Exergy analysis and exergy efficiency evaluation also serve for comparisons with other heating technologies [18].

Both air–water heat pumps and GSHPs are technologies employed for heating and cooling buildings, leveraging the heat pump principle to transfer heat from a low-temperature source to a high-temperature sink using a refrigerant. Both types have been examined from an exergy standpoint. For air–water heat pumps, studies such as Al-Sulaiman and Dincer [19] have examined the exergy efficiency of air–water heat pumps and evaluated the environmental impact associated with the use of these technologies. Al-Sulaiman and Hamdan [20] focused on an exergy analysis of an air–water heat pump, assessing the exergy efficiency of the system and identifying the main sources of exergy losses.

Similarly, investigations have explored the exergy efficiency and performance of geothermal heat pumps [21,22], as well the exergy losses of various components connected to building heating and cooling systems [23,24]. Additionally, Wang and Zhao [25] and Villafuerte and Coronas [26] conducted an exergy analysis of geothermal heat pump systems for building heating and cooling, gauging system exergy efficiency and comparing it with other heating and cooling technologies.

GSHPs utilize the ground's constant temperature as a heat source, while air–water heat pumps use the outside air as a heat source. Since the ambient air temperature can vary significantly, this can affect the efficiency of air–water heat pumps [27].

Cui, Zhao and Fang [28] and Sheng, Zhao and Wu [29] compared the performance of air–water and geothermal heat pumps in heating-dominated operation mode by analyzing the temperatures of heat sources and evaluating the system efficiency. Jeong, Jeong and Kang [30] addressed the performance disparities between geothermal and air–water heat pumps, factoring in outdoor air temperature fluctuations and their influence on heat source temperatures and system efficiency. The ground temperature also affects the design of the ground heat exchanger in geothermal heat pumps and consequently the system efficiency [31].

Compared to air–water heat pumps, GSHPs are often deemed more environmentally sustainable. Because the ground's temperature remains relatively constant year-round, geothermal heat pumps necessitate less energy to reach desired temperatures [32]. Bales and Ramesh [33] assessed the environmental performance of geothermal heat pumps in heating-dominated climates in North America, examining the benefits in terms of greenhouse gas emissions' reduction and the impact on energy and water consumption. Similar studies analyze the environmental and economic implications of air–water heat pumps in Chinese residential buildings, juxtaposed with other heating and cooling technologies, assessing their environmental advantages [34–36].

Within this context, this study endeavors to evaluate the energy systems of twelve residences situated in Rome, Italy. Exergy analysis is employed to evaluate the energy quality of the GSHP, photovoltaic system (PV), and solar collector (SC) proposed. Simultaneously, economic and environmental assessments are conducted. In summary, the study aims to (1) perform an exergy evaluation of an energy system comprising GSHP, PV and SC applied to a Rome building, (2) outline feasibility and environmental analyses. The Materials and Methods section (Section 2.1) outlines the characteristics and energy load demands of the case study. Section 2.2 describes the proposed energy system, while Section 2.3 applies an exergy evaluation to the energy system and its components, alongside economic analysis. Section 3 presents primary outcomes of the energy system, including exergy results, while the chief economic and environmental savings are detailed in Section 3.3.

## 2. Materials and Methods

### *2.1. Case Study and Energy Loads Evaluation*

The case study involves a building characterized by high energy performance (class A4 of the energy performance certificate) with a thermal performance index for winter conditioning of 25 kWh/m$^2$/year. This building is situated in Rome within climatic zone D, with a heating degree days (HDD) value of 1415. Comprising 12 flats, each apartment has a floor area of 90 m$^2$, and the operational schedule of the energy system adheres to regulations [37,38]. The heat generated by the GSHP serves two thermal purposes: it supplies the DHW thermal storage tank and fulfills the thermal demand for domestic heating during the winter operation. Throughout the summer period, the GSHP produces heat used for the DHW storage tank, and it subsequently utilizes the water mains as a cold source to facilitate summer cooling. The initial step involves calculating the total annual energy consumption for winter heating under the most severe conditions (Equation (1)), [37].

$$Q_w = \frac{ETh \cdot \left(T_{set\ point} - T_{min}\right)}{HDD} \quad (1)$$

where $T_{set\ point}$ is the temperature to guarantee inside the zone [37] and $T_{min}$ is the outside minimum temperature (0 °C), Figure 1. During the summer period, the technical plant must guarantee the indoor temperature equal to the summer set point temperature, assumed to be 26 °C (Equation (2)).

$$Q_s = \frac{ETh \cdot \left(T_{max} - T_{set\ point}\right)}{HDD} \quad (2)$$

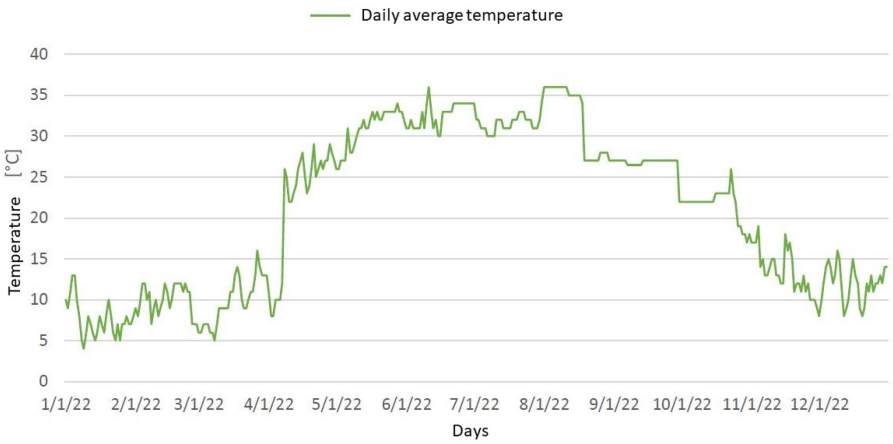


**Figure 1.** The annual temperature profile in Rome.

Moreover, the overall average efficiency of the heating system (downstream of the GSHP) is calculated as the product of the efficiency of the distribution system (95%), the efficiency of the heat emission system (with a radiator efficiency of 96%), and the efficiency of the regulation system (96%), resulting in a total of 87.5%. By dividing the $Q_w$ and $Q_s$

values with the global average efficiency and considering the surface (90 $m^2$) and operating hour of the thermal plant, the thermal and electrical power can be obtained.

The UNI 9182 [38] standard necessitates the definition of the duration of the "peak periods", contingent upon the specific type of user under consideration. Proper sizing of the heating system requires the DHW consumption calculation to be performed within these peak periods. For this scenario, the duration can be assumed to be 2 h.

The estimation of domestic hot water consumption is derived by considering the installed sanitary appliances and their frequency of utilization [38]. The calculation of the maximum hot water usage is carried out according to Equation (3), in which the numerator represents the consumption of each device (based on daily usage), while the total consumption is denoted in the denominator.

$$Q = \sum_{i=1}^{devices} \frac{Devices\ consumption \left[\frac{l}{use}\right]_i \cdot n^\circ\ of\ usage \left[\frac{use}{day}\right]_i \cdot n^\circ\ of\ devices}{consumption\ [\frac{h}{HDD}]_i} \quad (3)$$

The outcome corresponds to the peak identified by the apex of the dotted red line (approximately 0.2 kg/s at 19:00) in Figure 2. Subsequently, the daily DHW load profile was derived based on the typical patterns of domestic usage, resulting in the dashed red line (Figure 2). By employing an iterative approach to the daily load profile, the replenishment curve profile was established. The volume of water within the tank proved adequate to fulfill user demands, as indicated by the solid blue line in Figure 2. The simultaneity factor, established in relation to the number of dwellings considered, is set at 0.48. The comprehensive DHW load diagram is described in Figure 2.

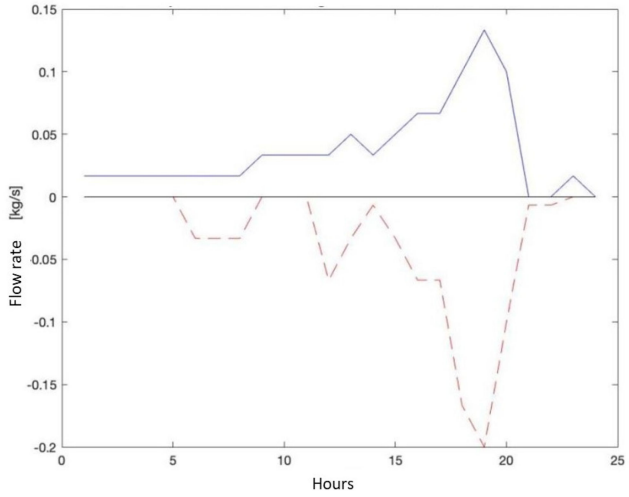


**Figure 2.** Profile of mass flow rates in thermal storage.

The daily DHW demands per user are approximately 260 L/day. The thermal storage tank necessitates a volume of 50 L. The daily filling pattern of the tank was computed and depicted in Figure 3 to validate the volumetric sizing. This was achieved by utilizing the daily load profiles (represented by the red dashed line in Figure 2) and replenishment profiles (depicted by the solid blue line in Figure 2).

To calculate the thermal power required for storage daily, it is necessary to define the operating conditions:

- Average daily temperature at the outlet of the accumulation tank equal to 318.15 K.
- Tank replenishment water temperature equal to 283.15 K in winter operating mode, and about 292 K in summer operating mode.
- Pressure of the make-up water entering the tank equal to 240 kPa.
- DHW pressure at tank outlet equal to 200 kPa.
- Overall heat-exchange coefficient of the tank equal to 2 W/K.

The energy balance equation referring to the heating (Equation (4)), takes into account the mass flows inlet/outlet and the thermal losses from the tank to the outside (Figure 4).

$$Q = Q_{HP} + Q_{solar} = m_{DHW} \cdot dh_{out} + m_{heating} \cdot dh_{in} + \frac{d}{dt}[\int e \cdot \rho \cdot dV] + Q_{loss} \quad (4)$$

where $Q$ is the daily trend of the required thermal power, composed of two different components such as $Q_{HP}$ (heat supplied by the GSHP) and $Q_{solar}$ (heat supplied by the solar collector); $m$ is the mass flow rate; $dh$ is the thermal power and $e$ is the specific energy contribution to the mass in the system; $\rho$ is the density of water contained in the tank; $dV$ is the variation in water's volume and $Q_{loss}$ is the thermal losses from the tank to the outside.

The temperature of the contents within the tank during the heat pump's operation (from 5:00 to 20:00) is maintained at 318.15 K. The system has been engineered to operate continuously throughout the day to mitigate fluctuations in temperature. Consequently, the daily trajectory of the necessary thermal power can be derived, as depicted in Figure 5.

Both winter and thermal losses (Figures 4–7) were calculated according to the following parameters:

– Overall heat transfer coefficient of the tank is 2 W/K.
– Ambient temperature.
– Temperature of the water mass within the boiler.

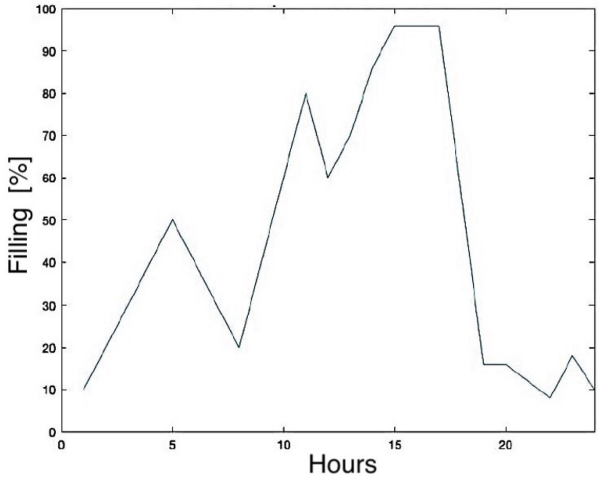


**Figure 3.** Daily store of thermal storage.

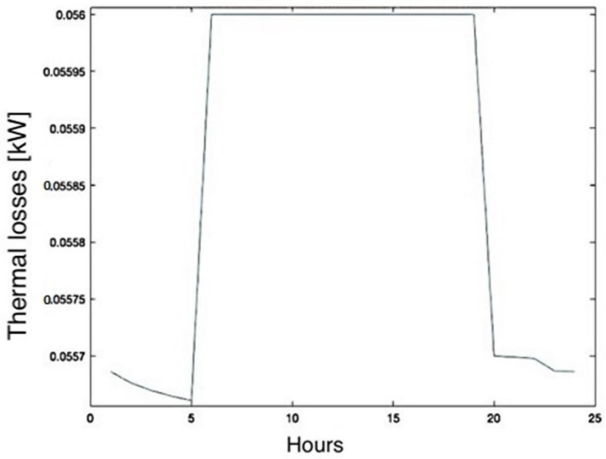


**Figure 4.** Losses towards the outside of the thermal storage.

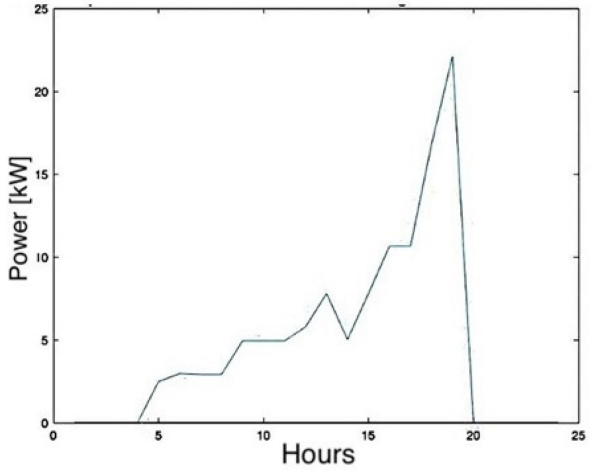


**Figure 5.** Thermal power is required for thermal storage in winter operating mode.

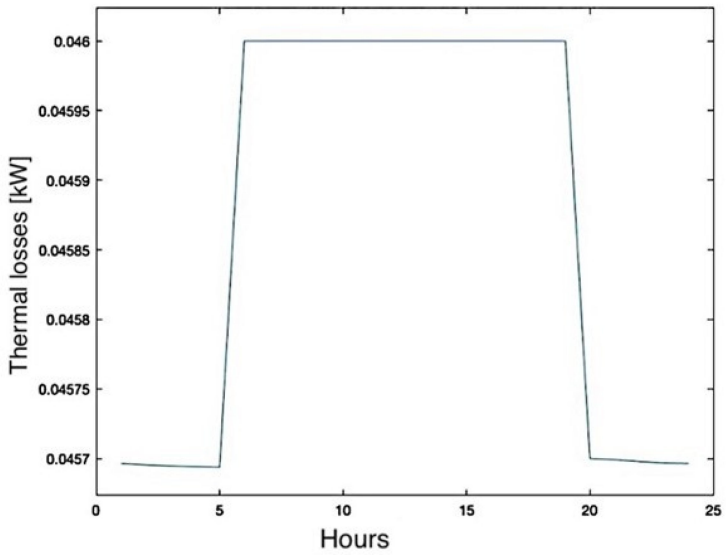


**Figure 6.** Losses towards the outside of the thermal storage during the summer period.

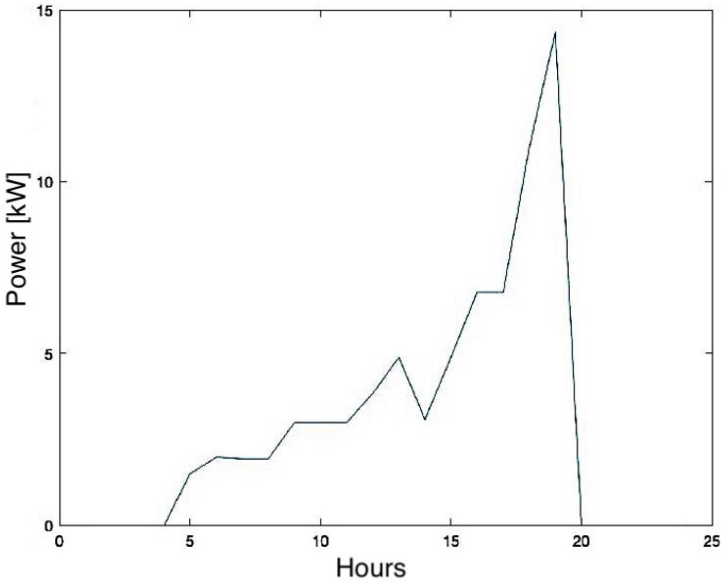


**Figure 7.** Thermal power is required for thermal storage in the summer period.

Since the aim of the project is the annual analysis of the average daily values proposed by the system, the average daily thermal load values of DHW are assumed to be constant during the year. These values have been calculated as 2/3 of the peak power (Figure 8).

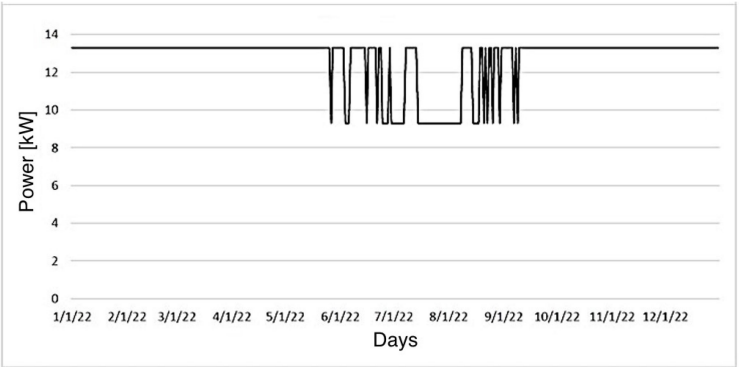


**Figure 8.** Average daily total thermal power required by the thermal storage.

### *2.2. Energy Plant Description*

The low enthalpy geothermal heat pump sends hot water to the users at a set temperature of 321.15 K. The system is regulated by controlling the mass flow from the GSHP, which varies according to the average daily heat requirement of the user. The COP of the GSHP is 5.8. The entire energy system is shown in Figure 9.

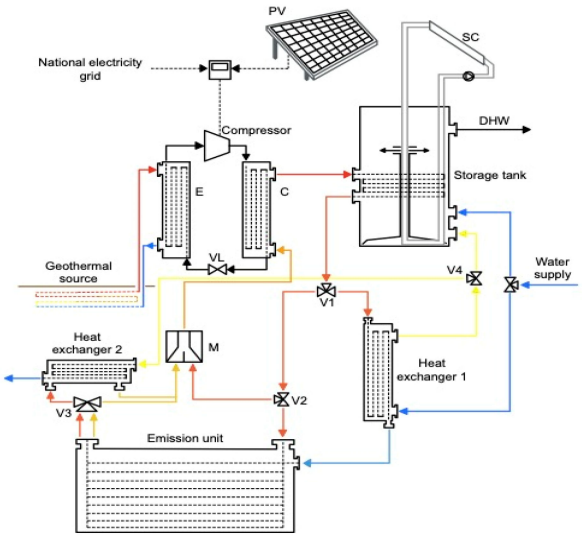


**Figure 9.** Technical layout plant.

The low enthalpy geothermal heat pump delivers hot water to users at a predetermined temperature of 321.15 K (Figure 9). The system is regulated by controlling variable mass flow in line with the user's average daily heat demand. The GSHP conveys the heat transfer fluid to the boiler, which is heated through a closed circuit, causing an imposed thermal drop of 4 K upon crossing the boiler. Simultaneously, the boiler receives thermal power from the solar thermal collector through a separate closed circuit to ensure fluid separation. The total thermal power supplied to the boiler facilitates the distribution of DHW to users via a specialized, unillustrated distribution system. Water replenishment within the storage occurs through two methods:

- During the winter season, heat exchanger 1 remains inactive, directing water directly from the "Water Supply" into the boiler.
- In the summer, the need for cooling mandates a reduction in the heat transfer fluid's temperature as it passes through the radiator. This cooling process transpires within

heat exchanger 1. The heat extracted from the fluid in heat exchanger 1 is repurposed for preheating water entering the boiler, aiding in reducing the overall thermal load. In this instance, replenishment occurs through the V4 valve.

In this case study, a vacuum solar collector is employed, possessing an absorption coefficient of $F_r$ = 0.94. The collector consists of 14 double-walled glass vacuum tubes, each enclosing a copper tube. These copper pipes are interconnected in parallel and traversed by a heat transfer fluid with a specific nominal mass flow of 0.008 kg/s·m$^2$. The overall heat transfer coefficient towards the external environment is 1.15 W/m$^2$K. The average daily solar radiation in Rome throughout the year is shown in Figure 10.

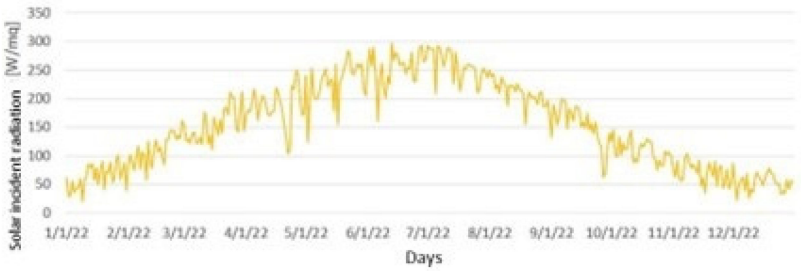


**Figure 10.** Average daily incident solar radiation.

Given a panel surface ($A_m$ = 2.7 m$^2$ per module), the energy flows to the solar thermal collector can be obtained using Equations (5)–(7).

$$Q_{sun} = F_r \cdot A * Rad_{sun} = F_r \cdot n_{mod} \cdot Rad_{sun} \quad (5)$$

where $F_r$ is the absorption coefficient of the vacuum solar collector; $A$ is the collector surface; $Rad_{sun}$ is the average solar radiation in Rome; $n_{mod}$ is the number of collector modules. The maximum surface available is 9 m$^2$ and $n_{mod}$ (number of the module) is three.

$$Q_{loss} = U \cdot A \cdot (T_{collector} - T_{outside}) \quad (6)$$

$$Q_{used} = Q_{sun} - Q_{loss} \quad (7)$$

where $Q_{loss}$ is the thermal power lost; $U$ is the transmittance of the panel and $Q_{sun}$ is the thermal power obtained from solar radiation incident on the collectors.

By setting the inlet temperature of the collector equal to the average daily temperature of the heat storage (45 °C), the outlet temperature from the collector is obtained. The energy efficiencies of the solar thermal collector are calculated using Equation (8).

$$\eta_{energy,solar\ collector} = \frac{Q_{out}}{Q_{absorbed}} \quad (8)$$

After calculating the thermal power provided by the solar source and the thermal power needed for the DHW thermal storage, it became feasible to assess the thermal power entering the boiler from the GSHP (Equation (9)) and the mass flow exiting the heat pump (Equation (10)). An aggregated thermal loss was identified at the outlet of the boiler, encompassing the inefficiencies of the heating system's distribution. Consequently, this mass flow experiences a marginal temperature reduction (Equation (11)), as illustrated in Figure 11.

$$Q_{boiler,HP} = Q_{boiler} - Q_{u,solar} \quad (9)$$

$$m_{out,HP} = \frac{Q_{boiler,HP}}{cp \cdot dT} \quad (10)$$

$$T = T_{out,Boiler} - \frac{Q_{loss,destroyed}}{cp \cdot m_{out,HP}} \quad (11)$$

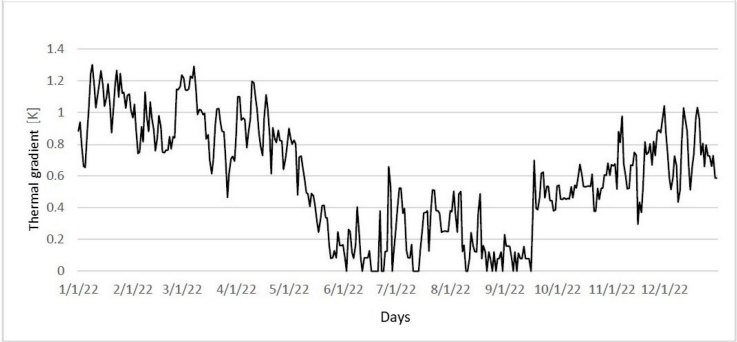


**Figure 11.** Concentrated thermal jump caused by inefficiencies of the distribution system.

To maximize the energy performance and enhance user self-consumption, the geothermal heat pump heating system is powered not solely by the national electricity grid but also by a photovoltaic panel system. In the case of monocrystalline silicon solar panels, the overall electrical system efficiency stands at 86%, while the panels have a TILT angle of 35° and an azimuth of 0°. Firstly, the average daily energy demand is established.

By considering the power demanded by the compressor and the daily operational hours of the heat pump (HP), it becomes possible to compute the average daily energy consumed. Then, to calculate the average energy produced daily, it is necessary to take into account the efficiency of the chosen module, which can be assumed equal to 18.5%. The average energy produced annually is then determined by multiplying the efficiency of the global electricity system, the efficiency of a single panel, and the average annual radiation on an inclined surface (1737.40 kWh/m$^2$ year). To calculate the installed kWp, i.e., the power extracted from the modules in standard conditions (1000 W/m$^2$ of irradiation, module temperature of 25 °C), it is enough to consider the efficiency of the system to pass from the STC (Standard Test Condition) to actual operating conditions.

### *2.3. Exergy and Economic Evaluations*

The exergy analysis of the plant was carried out following Equations (12)–(14).

$$EX_{Q0} = 0 \tag{12}$$

$$EX_Q = |Q| \cdot (1 - \frac{T_0}{T_{Hot}}) \tag{13}$$

$$EX_L = L \tag{14}$$

where $T_{Hot}$ is set to the flow temperature of the GSHP. Through the exergy balance equations [14], it is possible to calculate the annual average exergy efficiency (Equation (15)).

$$\varepsilon_{GSHP} = 1 - \frac{EX_{destroyed}}{EX_{fuel}} \tag{15}$$

The exergies related to the heat flows entering the boiler are the inlet exergy from solar thermal collector, GSHP and the outlet exergy from the boiler. Then, it was possible to calculate the exergy destroyed and the efficiency (Equation (16)).

$$EX_{distroyed} = EX_{in,boiler} + EX_{out,boiler} \tag{16}$$

The exergy efficiency of solar collector and heat exchanger is calculated as Equations (17) and (18), respectively.

$$\varepsilon_{solar\ collector} = \frac{EX(Q_{out})}{EX(Q_{absorbed})} \tag{17}$$

$$\varepsilon_{heat\ exchang.} = \frac{\left(1 - \frac{T_0}{T_{f,ML}}\right)}{\left(1 - \frac{T_0}{T_{c,ML}}\right)} \quad (18)$$

where $T_0$ is dead state temperature (15 °C); $T_{h,ML}$ and $T_{c,ML}$ are the temperatures hot- and cold-related to the heat exchanger.

At the inlet to the mixer are the flow rates $m_{mix}$, relative to the fluid with higher temperature ($T_{in,elem}$), and $m_{elem}$ output from the emission element at a lower temperature ($T_{in,elem}$, $dT_{elem}$). Table 1 reports the average values involve, where $h$ is enthalpy, $T$ is temperature, $s$ is heating capacity (Table 1).

**Table 1.** Enthalpy, temperature and heat capacity of mixers, emission element.

| $h_{element}$ [kJ/kg] | $h_{mixer}$ [kJ/kg] | $h_{out}$ [kJ/kg] | $T_{elem}$ [K] | $T_{mix}$ [k] | $T_{out}$ [K] | $s_{elem}$ [kJ/kg/K] | $s_{mix}$ [kJ/kg/K] | $s_{out}$ [kJ/kg/K] |
|---|---|---|---|---|---|---|---|---|
| 179.5 | 154.5 | 160 | 316 | 310 | 312 | 0.6 | 0.53 | 0.545 |

The exergy destroyed is described in Equation (19); then, the exergy efficiency can be evaluated, wherein $EX_{m,elem.}$ refers to the exergy of the considered element inside the system, while $EX_{m,out}$ refers to the exergy leaving the system.

$$EX_{distroyed} = EX_{m,mix} + EX_{m,elem.} - EX_{m,out} \quad (19)$$

To perform an economical evaluation, the marginal costs of the heating and cooling system will be analyzed to establish a quantitative comparison of the average annual cost compared to a conventional gas-fired heating system, and electricity (domestic air conditioners) for cooling requests. The traditional gas boiler has an energy efficiency of 90%, a PCI of 9.59 kWh/m$^3$ and the gas natural price is set to EUR 1.24/m$^3$ (ARERA). On the other hand, the price of electricity is EUR 0.361/kWh. Table 2 collects the cost of installation of each component employed within the system.

**Table 2.** Installation cost of the components listed.

| Component | Cost (EUR) |
|---|---|
| Horizontal probe | 5000 |
| HP and storage thank | 12,000 |
| Underfloor system | 60,000 |
| Heat exchanger and mixer | 1350 |
| Solar collector | 12,000 |
| Photovoltaic panels | 3,000,000 |

## 3. Results

### *3.1. Results of the Solar Collector, HP and PV Plant*

The ultimate winter and summer energy demands amount to 5.5 kWh/m$^2$ and 2.2 kWh/m$^2$, respectively. The thermal power profiles necessary for the system, along with losses accounting for inefficiencies in water distribution and heat transmission, are depicted in Figure 12. The average daily power absorbed by the solar collector is shown in Figure 13.

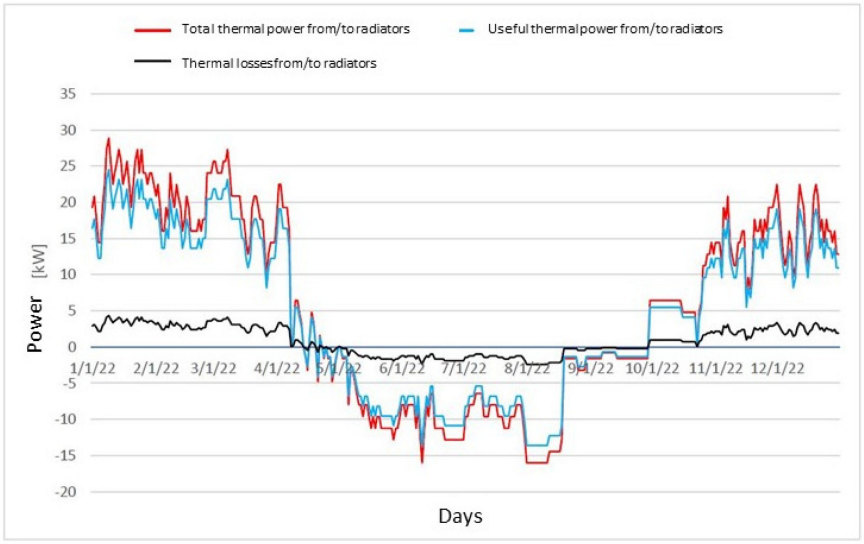


**Figure 12.** Power values to the emission element.

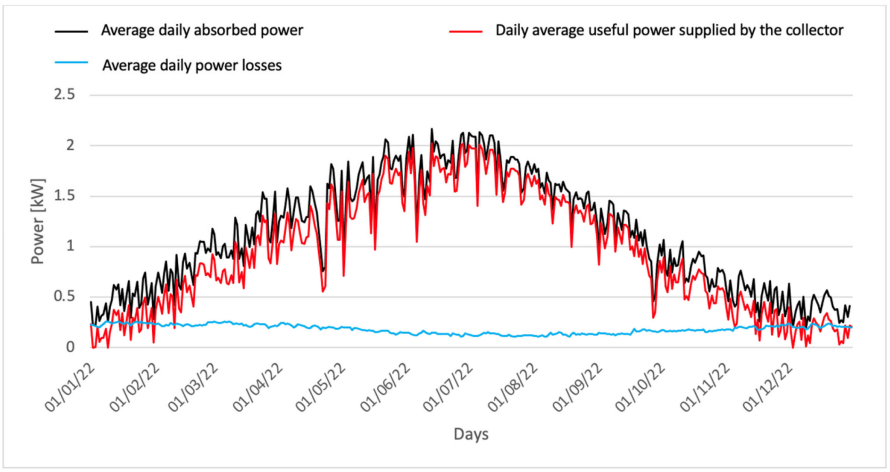


**Figure 13.** Energy flows to the solar thermal collector.

By setting the inlet temperature to the collector equal to the thermal accumulation's average daily temperature (45 °C), the resulting outlet temperature from the collector is determined (Figure 12). The annual average performance of the solar collector is 74.73%. The average power supplied to the storage tank and the mass flow deriving from the GHSP are reported in Figure 14. Figure 15 outlines the daily average energy fluxes of the GSHP.

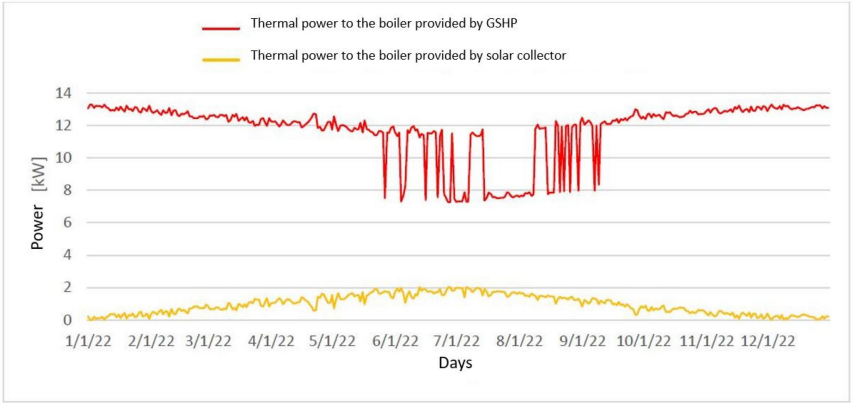


**Figure 14.** Average daily thermal power supplied to the thermal storage.

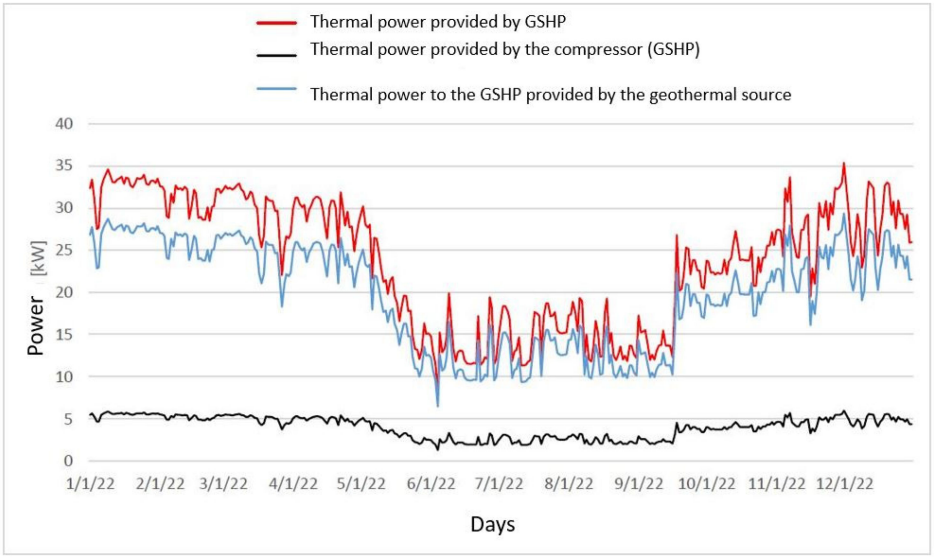


**Figure 15.** Powers exchanged by GSHP.

### *3.2. Results of Exergy Analysis*

Firstly, the exergy efficiency of each component of the systems is collected in Table 3.

**Table 3.** Installation cost of the components listed.

| Component | ε (%) |
|---|---|
| Photovoltaic system | 8.00 |
| HP and storage thank | 16.80 |
| GSHP | 64.30 |

The exergy efficiency of the GSHP is lower when compared to its energy efficiency (97.1%). This discrepancy arises from the dissipated exergy. The increase in exergy destruction within the system, signifying its inefficiency, is intricately tied to three factors:

- The temperature of the reference dead state.
- The COP of the heat pump.
- The external temperature (which influences the thermal power demanded by the user).

In this case the temperature of the dead state is constant, as we assume that the heat capacity of the soil is infinite. It can be assumed $EX_{destr}$ is a function of $T_{outside}$ and COP (Figure 16).

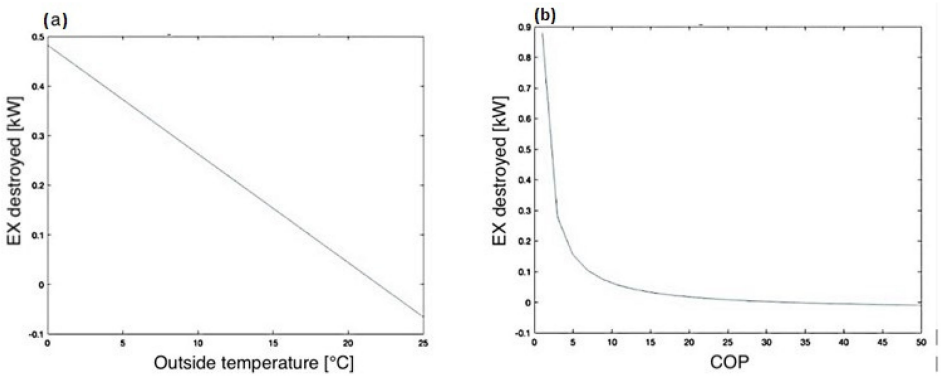


**Figure 16.** Variation in the destroyed exergy in function of (**a**) outside temperature and (**b**) COP.

As the COP increases to around 12, the value of exergy destruction experiences a significant reduction, followed by a more gradual decline. This behavior can be at-tributed to the coefficient of performance, which denotes the amount of mechanical power required to generate a specific quantity of thermal power. This phenomenon is characterized by the degradation of valuable energy, a degradation that diminishes as the COP of the machine increases.

Regarding the exergy destruction linked to ambient temperature, an increase in temperature corresponds to a linear decrease in exergy destruction. This phenomenon can be elucidated by the reduction in thermal energy, which, if generated from forms of mechanical energy, signifies a loss of thermodynamic efficiency. Furthermore, the breakdown of contributions from each system component to exergy destruction is presented in Figure 17.

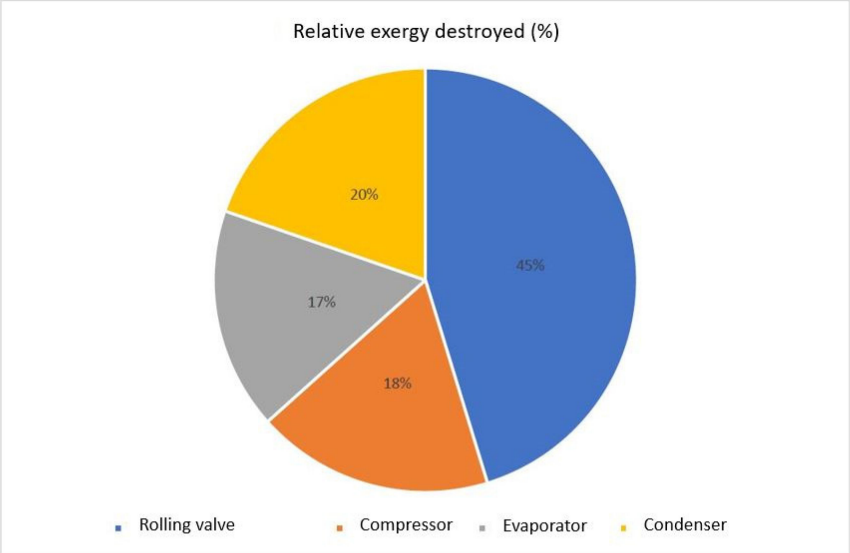


**Figure 17.** Relative exergy destroyed results of GSHP components.

The exergy destroyed and efficiency of both heat exchangers are reported in Table 4. The exergy efficiency of the mixer is 62%. The chart shown in Figure 18 compared the exergy efficiency of each component.

**Table 4.** Exergy destroyed and exergy efficiency of heat exchangers.

| Element | Exergy Destroyed | ε (%) |
|---|---|---|
| Heat exchanger 1 | 0.65 | 17.9 |
| Heat exchanger 2 | 0.43 | 21.7 |

The heat pump stands out with superior exergy efficiency, primarily due to its ability to generate thermal power at a higher temperature compared to the constant and relatively lower temperature of the dead state throughout the year, capitalizing on the heat capacity of the ground. The adiabatic mixer ranks as the second most exergetically efficient component, owing to the minimal logarithmic mean temperature difference between inlet fluids during year-round operation. In contrast, the two heat exchangers, which encounter higher thermal differentials, face drawbacks stemming from the irreversibilities inherent in heat exchange as the temperature variance between sources expands.

Photovoltaic panels, however, encounter notable constraints due to inherent material limitations; this results in considerably diminished energy efficiency, which subsequently reflects in their exergy efficiency.

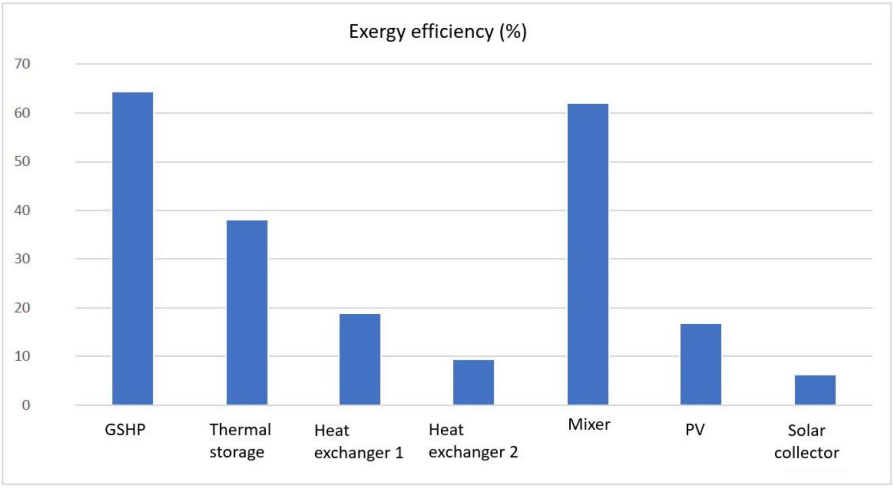


**Figure 18.** Exergy efficiency of each component of the energy plant.

### *3.3. Results of Economic Evaluation*

The annual gas consumption of the boiler chosen is equal to 6483.60 $m^3$/year for a cost of EUR 8039.67/year. Considering an EER of 3, the electricity demand is 913 kWh/year, for a cost of EUR 329.14/year. Moving to the DHW, the annual cost is EUR 8404.3/year. The total annual savings is around EUR 16,772/year. Based on the prices collected in Table 3, the total installation cost (PV not included) is EUR 390,350. The savings compared to the case of the conventional plant is equal to EUR 16,772 a, this means that the PBP is equal to 23 years.

The use of no fossil fuels in the plant implies a negligible $CO_2$ emission into the atmosphere. If we assumed for domestic heating an average emission factor derived from the use of natural gas equal to 1.95 kg $CO_2$ $m^3$, the average emissions into the atmosphere avoided are 2.85 $tCO_2$/year. During the summer period, the avoided emission account for 0.396 $tCO_2$/year, assuming a factor of 0.433 kg $CO_2$/kWh for a total of 26.2 $tCO_2$/year saved.

## 4. Conclusions

The predominant source of energy consumption within buildings arises from space conditioning, constituting approximately 60% of their overall energy usage. To mitigate the environmental footprint of buildings, the integration of renewable-energy systems like air-to-water heat pumps or geothermal heat pumps (GSHP) during the design phase can yield significant reductions. This study focus on the analysis of a heat pump serving a twelve-unit building situated in Rome. The investigation encompasses an energy/exergy analysis, supplemented by an eco-nomic evaluation, and culminates in an assessment of the system's environmental im-pact. To optimize energy performance and elevate user self-consumption, the geo-thermal heat pump heating system draws power not only from the national electricity grid but also from a photovoltaic panel system. Furthermore, a vacuum solar collector is considered for hot water generation. The system operates across two modes: summer and winter. During winter, the GSHP provides heat for domestic hot water (DHW) and space heating, while in summer, it supports DHW and facilitates cooling through the water network.

The exergy analysis reveals a substantial discrepancy between exergetic and energy efficiency. This outcome stems from the notable exergy destruction observed in the system. Further analysis dissects the exergetic performance of individual components, highlighting those with high efficiency and those that negatively impact overall exergetic efficiency. Notably, the heat pump demonstrates heightened exergetic efficiency, benefiting from its capacity to generate high-temperature thermal power in contrast to the constant and relatively low-temperature dead state. The adiabatic mixer follows as the second most

exergetically efficient component, trailed by two heat exchangers. The inherent material limitations of photovoltaic panels contribute to their relatively low energy efficiency, as evidenced in their exergetic efficiency.

Savings in comparison to a conventional plant configuration amount to EUR 16,772 per annum, equating to a Payback Period (PBP) of 23 years. Regrettably, substantial costs may deter widespread adoption, despite the notable thermal system efficiency. Nonetheless, the benefits extend beyond monetary savings, as the system's absence of fossil fuel usage translates to negligible (if any) $CO_2$ emissions. The system's annual average greenhouse gas emissions reduction tallies up to 26.2 metric tons of $CO_2$ per year. Future iterations of this study will explore extending the exergy analysis to an entire energy district, assessing the potential of GSHP and similar energy plants for the decarbonization process of urban settlements.

**Author Contributions:** Conceptualization, F.N., E.E. and R.F.; methodology, F.N., E.E. and R.F.; validation, F.N. and L.P.; data curation, F.N. and G.P.; writing—original draft preparation, F.N., L.P. and G.P.; writing—review and editing, L.P.; visualization, E.E. and F.N.; supervision, G.P. All authors have read and agreed to the published version of the manuscript.

**Funding:** This research received no external funding.

**Data Availability Statement:** No new data were created or analyzed in this study. Data sharing is not applicable to this article.

**Conflicts of Interest:** The authors declare no conflict of interest.

## References

1. European Commission. *Roadmap to a Competitive Low Carbon Economy in 2050*; COM (2011) 112 Final. Commission Communication; European Commission: Brussels, Belgium, 2011.
2. European Commission. *Draft Horizon 2020 Work Programme 2014–2015 in the Area of Secure, Clean and Efficient Energy*; European Commission: Brussels, Belgium, 2015.
3. Mauri, L.; Vallati, A.; Ocłoń, P. Low impact energy saving strategies for individual heating systems in a modern residential building: A case study in Rome. *J. Clean. Prod.* **2019**, *214*, 791–802. [CrossRef]
4. Schneider, S.; Zelger, T.; Sengl, D.; Baptista, J. A Quantitative Positive Energy District Definition with Contextual Targets. *Buildings* **2023**, *13*, 1210. [CrossRef]
5. van der Leer, J.; Calvén, A.; Glad, W.; Femenías, P.; Sernhed, K. Energy systems in sustainability-profiled districts in Sweden: A literature review and a socio-technical ecology approach for future research. *Energy Res. Soc. Sci.* **2023**, *101*, 103118. [CrossRef]
6. Pompei, L.; Nardecchia, F.; Bisegna, F. A new concept of a thermal network for energy resilience in mountain communities powered by renewable sources. *Sustain. Energy Grids Netw.* **2023**, *33*, 100980. [CrossRef]
7. Kim, S.; Kim, M. Exergy analysis of a ground-source heat pump system with horizontal ground heat exchangers. *Energy Build.* **2017**, *152*, 109–116.
8. Basso, G.L.; Pastore, L.M.; de Santoli, L. Power-to-Methane to Integrate Renewable Generation in Urban Energy Districts. *Energies* **2022**, *15*, 9150. [CrossRef]
9. González-Prieto, D.; Fernández-Nava, Y.; Megido, L.; Prieto, M.M. Economic and environmental prioritisation of potential retrofitting interventions in electricity decarbonisation scenarios: Application to a heritage building used as offices. *J. Build. Eng.* **2023**, *72*, 106561. [CrossRef]
10. Elaouzy, Y.; El Fadar, A. Investigation of building-integrated photovoltaic, photovoltaic thermal, ground source heat pump and green roof systems. *Energy Convers. Manag.* **2023**, *283*, 116926. [CrossRef]
11. Pompei, L.; Rosa, F.; Nardecchia, F.; Piras, G. The Environmental and Energy Renovation of a District as a Step towards the Smart Community: A Case Study of Tehran. *Buildings* **2023**, *13*, 1402. [CrossRef]
12. Pastore, L.M.; Basso, G.L.; Ricciardi, G.; de Santoli, L. Smart energy systems for renewable energy communities: A comparative analysis of power-to-X strategies for improving energy self-consumption. *Energy* **2023**, *280*, 128205. [CrossRef]
13. Júnior, J.A.; Sanches, A.O.; Martins, F.R. Exergetic analysis of a geothermal heat pump system. *Energy Procedia* **2018**, *152*, 398–405.
14. Pompei, L.; Nardecchia, F.; Mattoni, B.; Gugliermetti, L.; Bisegna, F. Combining the exergy and energy analysis for the assessment of district heating powered by renewable sources. In Proceedings of the 2019 IEEE International Conference on Environment and Electrical Engineering and 2019 IEEE Industrial and Commercial Power Systems Europe (EEEIC/I&CPS Europe), Genova, Italy, 11–14 June 2019; pp. 1–5. [CrossRef]
15. Groll, E.A.; Braun, J.E. Exergy analysis of air-source and ground-source heat pump systems. *Int. J. Energy Res.* **1994**, *18*, 369–383.
16. Ibrahim, M.M.; Al-Sulaiman, F.A. Exergy analysis of a ground-source heat pump system. *Energy Convers. Manag.* **2000**, *41*, 45–63.
17. Sopian, K.; Yatim, B. Exergy analysis of heat pump systems for drying applications. *Appl. Therm. Eng.* **2002**, *22*, 583–597.

18. Jeong, H.I.; Jeong, M.J. Comparative exergy analysis of a geothermal heat pump and an air source heat pump for space heating. *Energy* **2013**, *61*, 398–405.
19. Al-Sulaiman, F.A.; Dincer, I. Thermodynamic and environmental analysis of ground-source heat pump systems. *Appl. Therm. Eng.* **2002**, *22*, 185–194.
20. Al-Sulaiman, F.A.; Hamdan, M.A. Performance analysis of an air source heat pump using exergy. *Energy Convers. Manag.* **2009**, *50*, 53–59.
21. Hrnjak, P.; Braun, J.E. Exergy analysis of a ground-source heat pump system. *Energy* **1997**, *22*, 167–174.
22. Madani, H.; Ahmadi, M.H. Exergy analysis of a ground-coupled heat pump system with earth tube heat exchanger. *Energy Convers. Manag.* **2012**, *54*, 94–101.
23. Kwak, H.Y.; Kim, Y. Exergy analysis of a ground source heat pump system for heating and cooling applications. *Energy Build.* **2010**, *42*, 396–402.
24. Wang, R.Z.; Zhao, Y. Exergy analysis of a ground-source heat pump system for building heating. *Energy Build.* **2006**, *38*, 828–835.
25. Villafuerte, N.L.C.; Coronas, A. Exergy analysis of geothermal heat pump systems for heating and cooling of buildings. *Energy Build.* **2014**, *72*, 30–40.
26. Kilkis, B. Geothermal heat pump efficiency. *Appl. Energy* **2014**, *133*, 250–256.
27. Cui, X.; Zhao, L.; Fang, Z. Performance comparison of air source and ground source heat pump systems in heating-dominated operating mode. *Energy Build.* **2014**, *69*, 65–72.
28. Sheng, W.; Zhao, C.Y.; Wu, J.Y. Performance comparison of air- and ground-source heat pumps with different heat sources. *Energy Build.* **2011**, *43*, 3509–3517.
29. Jeong, S.; Jeong, M.; Kang, H. Comparative analysis of ground source and air source heat pumps considering the effects of air temperature variations. *Appl. Therm. Eng.* **2013**, *52*, 361–366.
30. Zeng, J.; Fang, Z.; Xu, Y. The influence of ground heat exchanger design on the performance of ground source heat pump systems. *Energy Procedia* **2017**, *142*, 1545–1550.
31. Lund, J.W.; Boyd, T.L. Direct utilization of geothermal energy 2015 worldwide review. *Geothermics* **2016**, *60*, 66–93. [CrossRef]
32. Bales, C.; Ramesh, G. Environmental performance of ground-source heat pumps in North American heating-dominated climates. *Renew. Energy* **2016**, *85*, 627–637.
33. Yang, M.; Zhai, Z.; Liu, G.; Li, N.; Fang, Z. Life cycle environmental and economic assessment of air source heat pumps for residential buildings in China. *Energy* **2018**, *163*, 699–707.
34. Zhai, Z.; Fang, Z.; Liu, G.; Li, N. Comparative life cycle assessment of ground source and air source heat pumps for residential buildings in China. *Energy Build.* **2016**, *129*, 183–190.
35. Wang, Y.; Yang, H.; Zhao, X. Life cycle energy and environmental analysis of ground source heat pump system: A case study of a residential building in Tianjin, China. *Renew. Energy* **2017**, *112*, 98–107.
36. *UNI 10339*; The Exchange of Air in Aeraulic Systems. Italian Organization for Standardization: Milan, Italy, 1995.
37. *UNI/TS 11300*; Reference Technical Standards for the Estimation of the Energy Performance of Buildings. Italian Organization for Standardization: Milan, Italy, 2014.
38. *UNI 9182*; The Technical Criteria, and Parameters to be Considered for the Sizing of the Distribution Networks of Water Intended for Human Consumption. Italian Organization for Standardization: Milan, Italy, 2014.